Original Paper

Early View publication on www.interscience.wiley.com (issue and page numbers not yet assigned; citable using Digital Object Identifier – **DOI**)

phys. stat. sol. (a), 1–5 (2007) / **DOI** 10.1002/pssa.200675352

Magnetotransport in high mobility epitaxial graphene

Claire Berger[*, 1, 3], **Zhimin Song**[1], **Xuebin Li**[1], **Xiaosong Wu**[1], **Nate Brown**[1], **Duncan Maud**[2], **Cécile Naud**[3], and **Walt A. de Heer**[1]

[1] School of Physics, Georgia Institute of Technology, Atlanta, Georgia 30332-0430, USA
[2] CNRS-LCMI, BP166, 38042 Grenoble cedex 9, France
[3] CNRS – Institut Néel, BP166, 38042 Grenoble cedex 9, France

Received 17 October 2006, revised 15 February 2007, accepted 15 February 2007
Published online 23 May 2007

PACS 73.20.–r, 73.23.–b, 73.43.Qt, 73.50.–h

Epitaxial graphene layers grown on single-crystal SiC have large structural coherence domains and can be easily patterned into submicron structures using standard microelectronics lithography techniques. Patterned structures show two-dimensional electron gas properties with mobilities exceeding 3 m^2/Vs. Magnetotransport measurements (Shubnikov–de Haas oscillations) indicate that the transport properties are dominated by the highly doped graphene layer at the silicon carbide interface. They reveal the Dirac nature of the charge carriers as predicted for a single graphene layer. The properties of Dirac fermions can be conveniently explored in epitaxial graphene with long electronic phase coherence at the micron scale.

1 Introduction

The discovery of fullerene and carbon nanotubes has spurred interest for graphitic materials. It was soon realized that carbon nanotubes have remarkable electronic properties, such as ballistic transport even at room temperature, quantum conductance, chirality and size – dependent electronic structure. Electronic structure calculations have in fact shown that these properties stem from the properties of graphene (a single layer of graphite), which constitute their basic structure. This has motivated us to develop ultra-thin graphite sheets and study their electronic properties [1, 2].

The key feature of the electronic structure of graphene is the presence of (only) two bands crossing at the Fermi level which have a linear dispersion relation: $E(k) = \hbar v_F k$ [3]. Contrary to normal systems, the velocity v_F is independent of energy, and electronic propagation in graphene can be regarded as propagation of light in a medium. This has interesting consequences on the transport properties. First is forbidden backscattering [3]. In 1D graphene systems, ballistic transport is therefore expected [4], as indeed observed in carbon nanotubes [5, 6]. In narrow ribbons of epitaxial graphene (width $\leq l_e$) we have presented evidence for long electronic mean free paths l_e and long phase coherence lengths [2]. Second, an anomalous Berry phase is predicted. This has given rise to quantum Hall effect plateaus at $n + 1/2$ values in exfoliated graphene, contrary to the usual integer magnetic field Landau quantization [7, 8]. The Landau spectrum has a characteristic square root dependence on magnetic field, which was also recently demonstrated in epitaxial graphene [9]. Evidence for the particular electronic structure of graphene and graphite was looked for in photoemission experiments [10–12].

We have recently found evidence that the magneto-transport properties of ribbons of ultra-thin graphite epitaxially grown on single crystal wafers of SiC are those of graphene, with anomalous Berry's phase, energy independent velocity $v_F = 10^6$ m/s, as calculated and as observed in exfoliated single

* Corresponding author: e-mail: berger@electra.physics.gatech.edu

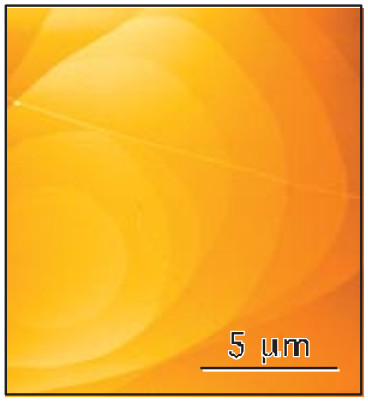

Fig. 1 (online colour at: www.pss-a.com) AFM picture of extended flat graphitized terraces. Graphene layers drape over the SiC substrate steps.

layer graphene. The long mean free path, high electronic coherence and high mobility (larger than 2.5 m^2/Vs), yielding electronic confinement in our narrow patterned ribbons, most certainly also stem from the char- acteristic electronic structure of graphene. The purpose of this paper is to extend the previous measurement to higher field and lower temperature.

2 Graphene growth and structural characterization

Epitaxial multilayer graphene is thermally grown in vacuum on the $000\bar{1}$ face of diced commercial SiC wafers after surface flattening by hydrogen etching [1, 2, 13]. After evaporation of metal contacts (Pd, Au), the films are patterned with an electron-beam and oxygen etched to define Hall bar structures.

The structure of the films is characterized by various surface tools in ultra high vacuum. As evidenced from low energy electron diffraction, an ultrathin graphite layer grows epitaxially on the SiC surface. X-ray diffraction reveals a thickness of 5–10 layers, and that graphene grown on the $(000\bar{1})$ face has a structural coherence larger than 300 nm [14, 15]. STM measurements show the $6\sqrt{3}\times 6\sqrt{3}$ reconstruction of the graphene on the SiC(0001) surface while the scanning tunneling spectroscopy measurements show the graphitic band structure and that the graphene layers grow over steps on the SiC surface. Extended terraces of tens of micrometers are routinely measured by atomic force microscopy (AFM) under ambient conditions, as shown in Fig. 1.

3 Transport experiments

High field measurements have been performed up to 23 Tesla at the High Magnetic Field Laboratory – CNRS in Grenoble in a dilution refrigerator. Here we present results on a Hall bar sample (1 µm × 6.5 µm) measured in a four-probe configuration with a lock-in technique.

The dependence of the square resistance ρ_{xx} on magnetic field at 180 mK is presented in Fig. 2. The magnetoresistance shows maxima (Shubnikov de Haas (SdH) oscillations), which are clearly seen after a smooth background subtraction (Fig. 2). A maximum occurs in the resistance at field B_n when the Fermi energy E_F crosses a quantized energy level E_n in field. In graphene: $E_n(B) = \sqrt{2neBv_0^2\hbar}$ [16], and hence $B_n = B_0/n$, where $B_0 = E_F^2/(2ev_0^2\hbar^2) = \hbar k_F^2/2e$. Each maximum is labeled with n and plotted as a function of $1/B_n$ in a Landau plot (inset of Fig. 2). The well identified peaks ($n = 2$–15) (the second quantum level is reached at 20 T) define a straight line: $B_n^{-1} = (n + \gamma)\, B_0^{-1}$. From the slope we define k_F and $n_s = 4k_F^2/4\pi = 3.7 \times 10^{12}$ carriers/cm^2, and the intercept at zero $\gamma = 0 \pm 0.09$ is consistent with previous experiment [2].

The two magnetoresistance traces for upward and downward magnetic field sweeps are reproducible down to the finest features (better than 0.1% at low field $B < 10$ T). This is exemplified at low field in Fig. 3 where a smooth background was subtracted from the resistance data $R_{xx} = \rho_{xx} \times$ length/width. Note in particular the reproducible resistance fluctuations at fine scale and the zero field resistance peak.

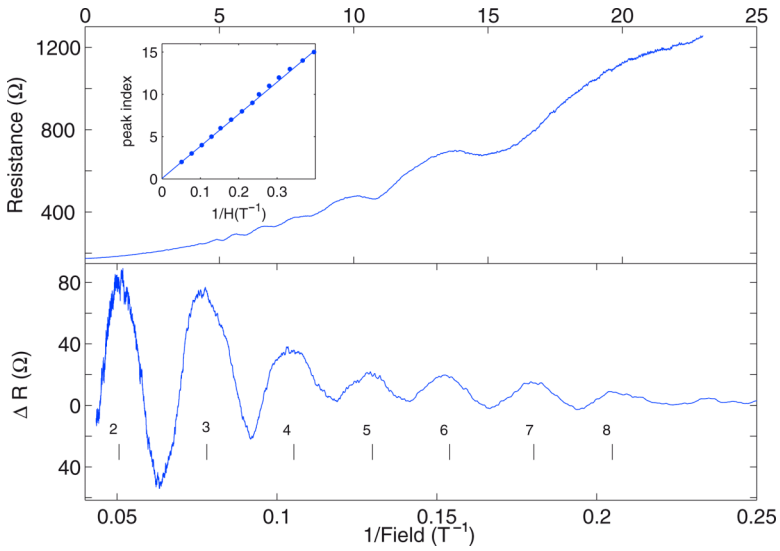

Fig. 2 (online colour at: www.pss-a.com) Top panel: Square resistance ρ_{xx} as a function of magnetic field at 180 mK showing the Shubnikov de Haas oscillations. Bottom panel: ρ_{xx} with a smooth background subtracted. The magnetoresistance peaks at B_n are labeled with their Landau level index n. Inset: Landau plot: n versus $1/B_n$ is a straight line, which intercepts the y-axis at $\gamma < 0.1$, consistent with a Berry phase $\Phi = \pi$, the slope gives a carrier density $n_s = 3.7 \times 10^{12}$ cm^{-2}.

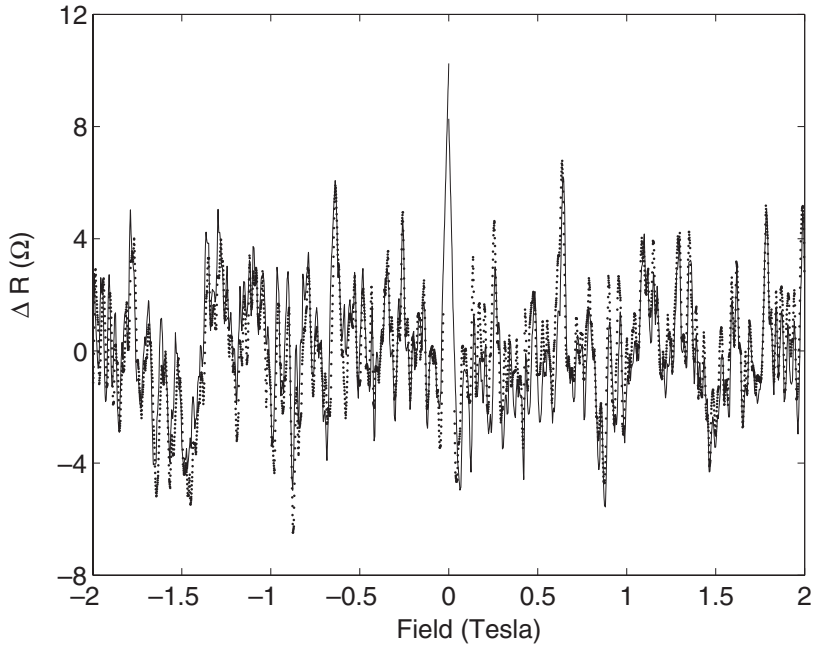

Fig. 3 Low field dependence of the resistance on magnetic field with a line subtracted (at 180 mK). It shows the reproducibility of the universal conductance fluctuations and the zero field weak localization peak. Full line: trace upward in field, dotted line, trace downward.

By attributing the peak to 2D weak localization, we estimate a phase coherence length $L\varphi$ of the order of 0.7 μm (this is a lower bound due to the low resolution of the very low field data). This estimate is consistent with the amplitude of the universal conductance fluctuations (UCF) $\Delta R_{\mathrm{UCF}} \approx 5\ \Omega$, i.e. $\Delta G_{\mathrm{UCF}} \approx 0.1 e^2/h$.

4 Discussion

The high-field low-temperature data nicely confirm previous results obtained for a narrow ribbon of epitaxial multilayer graphene. At low temperature, the SdH peaks can in principle be separated from the UCF peaks by their temperature dependence. The UCFs decay in temperature with a function of $(L\varphi/L)$, with $L\varphi \approx T^{\mathrm{p}}$. The amplitude of the SdH peaks varies according to the Lifshitz–Kosevich equation: $A(T)/A_0 = u/\sinh(u)$ where $u = 2\pi^2 k_{\mathrm{B}} T/\Delta E(B)$ and $\Delta E(B)$ is the separation between the energy level in field. At the resistance maxima $\Delta E(B) = E(B_n) - E_{\mathrm{F}}$, so that $\Delta E(B) \approx E_{\mathrm{F}}/2n$ proportional to B for Dirac electrons. Confinement was clearly identified in a 500 nm width ribbons by finding $\Delta E(B)$ essentially constant with field at low field. This is not expected to be the case here in a wider ±2D ribbon ($L\varphi \leq W$).

From the square resistance $\rho_{xx} = 175\ \Omega$, and the carrier density $n_{\mathrm{s}} = 3.7 \times 10^{12}\ \mathrm{cm}^{-2}$ we deduce a mobility $\mu = 1/(en_{\mathrm{s}}\rho_{xx}) = 0.95\ \mathrm{m}^2/\mathrm{Vs}$, a diffusivity $D = 0.1$ m/s and an electronic mean free path $l_{\mathrm{e}} = 2D/v_{\mathrm{F}} \approx 200$ nm. High mobility values in the range 1–3 m^2/Vs are commonly observed in our samples. Remarkably, narrow ribbons down to 50 nm retain a high mobility. More precisely, the resistance of narrow ribbons is often observed to be in the range of the ballistic resistance, as defined by $R = 1/(4Ne^2/h)$, with the number of channels $N = k_{\mathrm{F}}W/\pi$ depending on the width W. This indicates that even narrow ribbons keep long electronic mean free paths.

The relatively large carrier density corresponds to $E_{\mathrm{F}} = 2500$ K, which is consistent with the estimate of E_{F} from the analysis of the temperature dependence of the SdH peaks [2] and from photoemission data ($E_{\mathrm{F}}/k_{\mathrm{B}} = 2700$ K for 2 EG layers on (0001)SiC) [12]. Also Hall effect measurements indicate that carriers are electrons, in agreement with *ab initio* calculations of graphene layers in epitaxy on SiC [17].

The carrier density is remarkably constant from sample to sample. Note that besides the patterning, no subsequent treatment is applied to the samples after graphitization. We have measured many samples showing SdH oscillations with little (less than 10%) variation in n_{s} from sample to sample. In fact a carrier density of $n_{\mathrm{s}} \sim 1 \times 10^{12}$ electrons/cm^2 is consistent with a charge density at the interface producing an electric field to compensate the work-function difference between the materials. Only the interface layer is expected to be significantly charged [18, 19]; the other layers are essentially neutral. Infrared Landau level spectroscopy [9] indeed reveals the presence of neutral graphene layers of density $n_{\mathrm{s}} \approx 10^{10}$ carriers/cm^2. Therefore we believe that the electronic transport in ribbons is dominated by the layer at the interface.

The SdH oscillations are consistent with doped graphene. In agreement with our previous observation in epitaxial graphene in a smaller magnetic field range (0–9 T) [2], the Landau plot of Fig. 2 gives $\gamma = <0.1$, consistent with a Berry's phase of π. It is specifically not consistent with $\gamma = \pm 0.5$ as would be the case for normal electrons. This γ value is expected for graphene [16], and has been observed in exfoliated single graphene layers [7, 8]. Our observation seems at first surprising in a system which consists of several layers. Recent calculations indeed show that the electronic structure of stacked uncharged graphene layers can vary significantly with the number of layers and the stacking order [20]. We first note that we have indication that the transport in our sample is essentially dominated by the interface layer. Second, X-ray diffraction studies [15] and IR Landau spectroscopy [9] indicate that multi-layered epitaxial graphene resembles more a stack of independent graphene layers than regular Bernal stacked graphite. IR spectroscopy clearly demonstrate that the Landau energy level spectrum of the neutral layers varies as $\sqrt{B}$, like single graphene layers and with a velocity v_{F} that of graphene (10^6 m/s), indicating unambiguously that the system does not behave like graphite.

Acknowledgements Supported by NSF-NIRT grant 0404084, and NSF-MRI grant 0521041, a grant from Intel Research Corporation, and a USA-France travel grant from CNRS. We acknowledge discussions with D. Mayou and J. D. Meindl.

References

[1] C. Berger, Z. Song, T. Li, X. Li, A. Y. Ogbazghi, R. Feng, Z. Dai, T. Grenet, A. N. Marchenkov, E. H. Conrad, P. N. First, and W. A. de Heer, J. Phys. Chem. B **108**, 19912 (2004).
[2] C. Berger, Z. Song, X. Li, X. Wu, N. Brown, C. Naud, D. Mayou, T. Li, J. Hass, A. N. Marchenkov, E. H. Conrad, P. N. First, and W. A. de Heer, Science **3012**, 1191 (2006).
[3] T. Ando, T. Nakanishi, and R. Saito, J. Phys. Soc. Jpn. **67**, 2857 (1998).
[4] C. T. White and T. N. Todorov, Nature **393**, 240 (1998).
[5] S. Frank, P. Poncharal, Z. L. Wang, and W. A. de Heer, Science **280**, 1744 (1998).
[6] W. Liang, M. Bockrath, D. Bozovic, J. H. Hafner, M. Tinkham, and H. Park, Nature **411**, 665 (2001).
[7] K. S. Novoselov, A. K. Geim, S. V. Morozov, D. Jiang, M. I. Katsnelson, I. V. Grigorieva, S. V. Dubonos, and A. A. Firsov, Nature **438**, 197 (2005).
[8] Y. B. Zhang, Y. W. Tan, H. L. Stormer, and P. Kim, Nature **438**, 201 (2005).
[9] M. Sadowski, G. Martinez, M. Potemski, C. Berger, and W. A. de Hee, Phys. Rev. Lett. **97**, 266405 (2006).
[10] S. Y. Zhou, G.-H. Gweon, J. Graff, A. V. Fedorov, C. D. Sparatu, R. D. Diehls, Y. Kopelevic, D.-H. Lee, S. G. Louie, and A. Lanzara, Nature Phys. **2**, 595 (2006).
[11] T. Ohta, A. Bostwick, T. Seyller, K. Horn, and E. Rotenberg, Science **313**, 951 (2006).
[12] E. Rollings, G.-H. Gweon, S. Y. Zhou, B. S. Mun, J. L. McChesney, B. S. Hussain, A. V. Fedorov, P. N. First, W. A. de Heer, and A. Lanzara, J. Phys. Chem. Solids **67**, 2172 (2006).
[13] I. Forbeaux, J. M. Themlin, and J. M. Debever, Phys. Rev. B **58**, 16396 (1998).
[14] J. Hass, C. A. Jeffrey, R. Feng, T. Li, X. Li, Z. Song, C. Berger, W. A. de Heer, P. N. First, and E. H. Conrad, Appl. Phys. Lett. **89**, 143106 (2006).
[15] J. Hass, R. Feng, J. Millàn-Otoya, X. Li, M. Sprinkle, P. N. First, C. Berger, W. A. de Heer, and E. H. Conrad, Cond-mat/0702540, Phys. Rev., in print.
[16] S. G. Sharapov, V. P. Gusynin, and H. Beck, Phys. Rev. B **69**, 075104 (2004).
[17] F. Varchon, J. Hass, R. Feng, B. Ngoc Nguyen, X. Li, C. Naud, P. Mallet, J.-Y.Veuillen, C. Berger, E. H. Conrad, and L. Magaud, Phys. Rev. Lett., submitted.
[18] P. B. Visscher and L. M. Falicov, Phys. Rev. B **3**, 2541 (1971).
[19] B. Zhang, J. P. Small, M. E. S. Amori, and P. Kim, Phys. Rev. Lett. **94**, 176803 (2005).
[20] F. Guinea, A. H. Castro Neto, and N. M. R. Peres, Phys. Rev. B **73**, 245426 (2006).

